International Knowledge Centre for Engineering Sciences and Technology under the Auspices of UNESCO
联合国教科文组织国际工程科技知识中心

Disaster Risk Reduction Knowledge Service
防灾减灾知识服务

Scientific and Technological Trend Report in the Field of Disaster Risk Reduction

——Bibliometric analysis of global disaster risk reduction literature and the influence of Chinese research in 2019

Institute of Geographic Sciences and Resources Research, Chinese Academy of Sciences
National Science Library, Chinese Academy of Sciences
IKCEST Disaster Risk Reduction Knowledge Service System
2019.12

Abstract

As of December 30, 2019, a total of 6,312 SCI journal papers in disaster risk reduction field, which were published in 2019, were retrieved and interpreted by experts. Moreover, a total of 143 countries have carried out relevant research in this field. The most noteworthy specifics among these papers are outlined as follows:

——The top 13 countries with more than 200 papers are: China, the United States of America, the United Kingdom, Italy, Germany, India, Australia, Canada, Japan, France, Spain, Iran and South Korea. Amongst all countries, China has the largest number of publications.

——The institute of Ist Nazl Geofis & Vulcanol, located in Italy, and the United States Geological Survey have the highest cited rate, with more than 75% of papers being cited by these establishments. The institutions with the highest paper cited rate in China are the Chengdu University of Electronic Science and the Technology of China and Chinese Academy of Sciences.

——The papers are mainly distributed in 11 disciplines and are composed of more than 300 papers. The 11 disciplines include: Environmental Science, Geoscience Multidisciplinary, Water Resources, Meteorology and Atmospheric Science, Geochemistry and Geophysics, Public Environment and Occupational Health, Engineering Geology, Engineering Environment, Remote Sensing, Geography, and Natural Environment Research. The research on disaster prevention in China covers 68 subject areas, but is mainly focused on the following 10 disciplines (with more than 100 papers): Environmental Science, Geoscience Multidisciplinary, Water Resources, Meteorology and Atmospheric Sciences, Engineering Geology, Engineering Environment, Green and Sustainable Technology, Public Environment and Occupational Health, Remote Sensing, and Environmental Research. In the field of disaster prevention in China, there has been little research conducted on Geochemistry and Geophysics, nor Geography.

——The five hot topics of research consist of: toxic emissions

and environmental pollution disasters, the study on the mechanism of earthquake and landslide disasters, model simulation of surface movement, risks of climate change, and social adaptability, temperature, and extreme weather.

——As shown in the appendix, 48 abstracts of papers with high cited rates, and those close to the Disaster Risk Reduction Knowledge Service System of International Knowledge Centre for Engineering Sciences and Technology (IKCEST), are selected.

Contents

Developed in recent years, bibliometrics is a branch of the Library and Information Sciences that uses mathematical and statistical methods to describe, evaluate, and predict the current situation and development trend of science and technology, with the help of various characteristic quantities of literature. The Web of Science (WOS) core collection database of the Institute for Scientific Information of the United States includes the best scientific and technological journals from various disciplines throughout the world. To a certain extent, the papers included in this database can reflect the development trend of the scientific frontier, as well as the state and the publication situation of countries and institutions in certain periods of time. Furthermore, it can reflect the dominant position of each country and institution in a certain discipline. Based on the data from the WoS core collection database, the InCites database integrates the "Analytical Integrated Indicator System," [1] as well as the key indicators of Essential Science Indicators (ESI) and journal city report (JCR). An analysis of this data can fully reveal the academic competitiveness of countries and institutions in various subject areas.

Through bibliometric analysis, this research asserts the paper output and influence of the major countries and research institutions in the field of disaster risk reduction science. Furthermore, the hot papers within the research areas are discovered, and the advantages and disadvantages of research in China are analyzed. This is undertaken to grasp the development trend of scientific research on disaster risk reduction at a macro level.

[1] http://help.incites.clarivate.com/inCites2Live/8980TRS/version/default/part/AttachmentData/data/InCites-Indicators-Handbook%20-%20June%202018.pdf

1. Distribution of research capability

1.1 Output and influence of papers in major countries

Combined with expert interpretation, as of the retrieval date[2], the searchers have found 6,312 SCI journal papers in disaster risk reduction field that were published in 2019, and found 143 countries to have carried out relevant research in this field. The top 13 countries with more than 200 papers are: China, the United States of America, the United Kingdom, Italy, Germany, India, Australia, Canada, Japan, France, Spain, Iran and South Korea. On a global scale, China has the largest number of publications in the world, with a total of 1,714 papers having Chinese participation, accounting for about 27.2% of the total papers and occupying a leading position in this research field. The number of papers in the United States ranks second, accounting for about 21.5% of the total papers (Table 1).

Among the top 13 countries, Chinese and American papers are cited the most frequently[3], but the cited rate of American papers is one quarter higher than that in China. With this said, Italian and Iranian papers have a higher cited rate, with more than 75% of the papers being cited. Moreover, Italian and Korean papers are cited at a higher frequency, with an average of 7.0 times. Australia has a higher proportion of high-cited papers, both exceeding 1.5%, which is much higher than the proportion of high-cited papers in the top 10 countries. Furthermore, Iran, Italy, and South Korea have the highest percentage of hot papers[4], which is greater than the average value of the top 13 countries in this respect. This indicates that these three countries have produced a considerable number of high-level achievements in the last year, and have attracted the attention of

[2] December 30, 2019
[3] Web of Sciences, Core collection cited frequency
[4] http://help.incites.clarivate.com/inCites2Live/8980TRS/version/default/part/AttachmentData/data/InCites-Indicators-Handbook%20-%20June%202018.pdf

world scientists (see Table 1).

It is worth noting that Iran has participated in a relatively small number of scientific research publications, but the papers are cited at a high frequency, the cited rate of the papers is high, and the scientific research efficiency is high. In contrast, although China participated in a large number of scientific research publications, the average cited frequency of the papers is relatively low, the cited rate of the papers is low, and the efficiency of scientific research is low (see Figure 1).

Table 1 The top 10 countries for the number of papers on disaster prevention research in SCIE database and their influence.

Ranking	Country	Publication Mount	Proportion of cited Papers (%)	Time of Cited	Cited of Frequency	ESI Highly Cited Paper%
1	China	1714	38.04	1916	1.12	1.23
2	U.S.A	1356	41.59	1396	1.03	0.74
3	Britain	505	46.14	526	1.04	0.40
4	Italy	442	48.87	619	1.40	1.58
5	Germany	348	45.69	462	1.33	1.15
6	India	334	37.72	334	1.00	0.90
7	Australia	322	40.68	428	1.33	2.48
8	Canada	286	43.01	366	1.28	1.05
9	Japan	277	38.99	358	1.29	1.44
10	France	263	39.92	259	0.98	1.52
11	Spain	249	46.59	333	1.34	0.80
12	Iran	233	47.21	574	2.46	6.01
13	Korea	213	37.56	299	1.40	2.35
Average		503.23	42.46	605.38	1.31	1.67

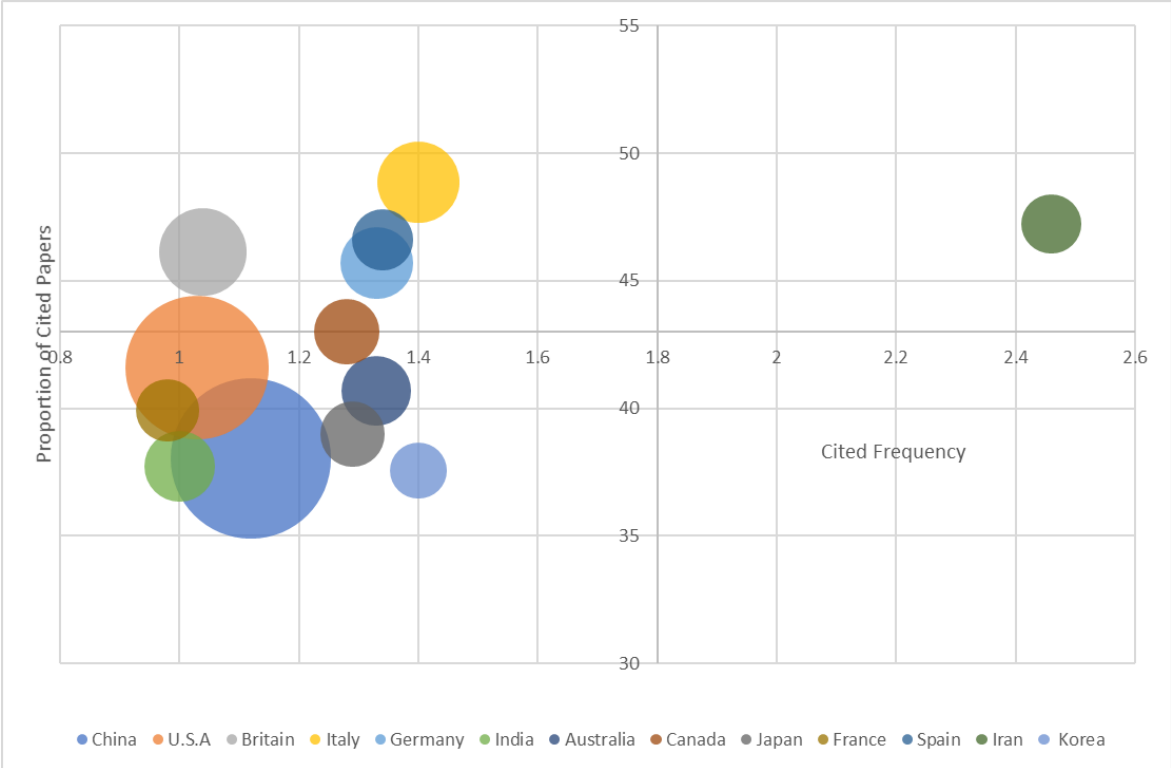

Figure 1 The total number of papers, the cited frequency of the papers and the proportion of cited papers in each country.

1.2 Output and influence of papers of main research institutions

By analyzing the top 10 institutions with the highest number of papers published by the first author, we see that China has the largest number of institutions (8/10), accounting for about 10% of the total publications. This indicates that the relative concentration of research in this field is conducted in China. The two top 10 institutions that are not Chinese are the institute of Ist Nazl Geofis and Vulcanol, located in Italy, and the United States Geological Survey, which has the highest cited rate. Of the papers found, more than 75% of these papers are cited. The institutions with the highest paper cited rate in China are the Chengdu University of Electronic Science and the Technology of China and Chinese Academy of Sciences. The cited frequency of the papers of the United States Geological Survey is much higher than the average level of the top 10 countries, indicating a higher average output quality. The three

papers that are cited more than 10 times are as follows: (1) Construction of probabilistic event trees for eruption forecasting at Sinabung volcano, Indonesia 2013-14, (2) Using a process-based model of pre-eruptive seismic patterns to forecast evolving eruptive styles at Sinabung Volcano, Indonesia, and (3) Monitoring, forecasting collapse events, and mapping pyroclastic deposits at Sinabung volcano with satellite imagery. Only two Chinese institutions, the China University of Geosciences and the Chengdu University of Electronic Science and Technology, are cited more frequently than the average cited frequency of the top 10 countries (see Table 2).

Among the top 10 paper posting institutions, there is only one high-cited paper, which is published by the Chinese Academy of Sciences. The title of this high-cited paper is "Recent Third Pole's Rapid Warming Accompanies Cryospheric Melt and Water Cycle Intensification and Interactions between Monsoon and Environment: Multidisciplinary Approach with Observations, Modeling, and Analysis". While this paper is high-cited, the Chinese Academy of Sciences has a large number of zero-cited papers, thus, making the average research level of the Chinese Academy of Sciences inferior to that of university research institutions in other countries.

It is worth noting that the papers published by the United States and Geological Survey are all cited at high frequency and at a high rate. Moreover, the scientific research efficiency of the United States Geological Survey is significantly higher than that of other institutions (see Figure 2).

Table 2 The top 10 institutions for the number of papers on disaster prevention research in SCIE database and their influence

Ranking	Institutions	Country	Publication Mount	Proportion of cited Papers (%)	Time of Cited	Cited of Frequency
1	**Chinese Academy of Sciences**	China	189	38.62	182	0.96
2	**China University of Mining and**	China	50	38.00	34	0.68

	Technology					
3	**China Seismological Bureau**	China	42	28.57	28	0.67
4	**Ist Nazl Geofis & Vulcanol**	Italy	42	40.48	38	0.90
5	**US Geol Survey**	U.S.A	39	56.41	71	1.82
6	**Beijing Normal University**	China	35	34.29	29	0.83
7	**China University of Geosciences**	China	35	31.43	35	1.00
8	**WuHan University**	China	32	31.25	29	0.91
9	**Chengdu Electronic Technology University**	China	30	40.00	44	1.47
10	**Nanjing University of information technology**	China	29	34.48	22	0.76
Average			52.30	37.35	51.20	1.00

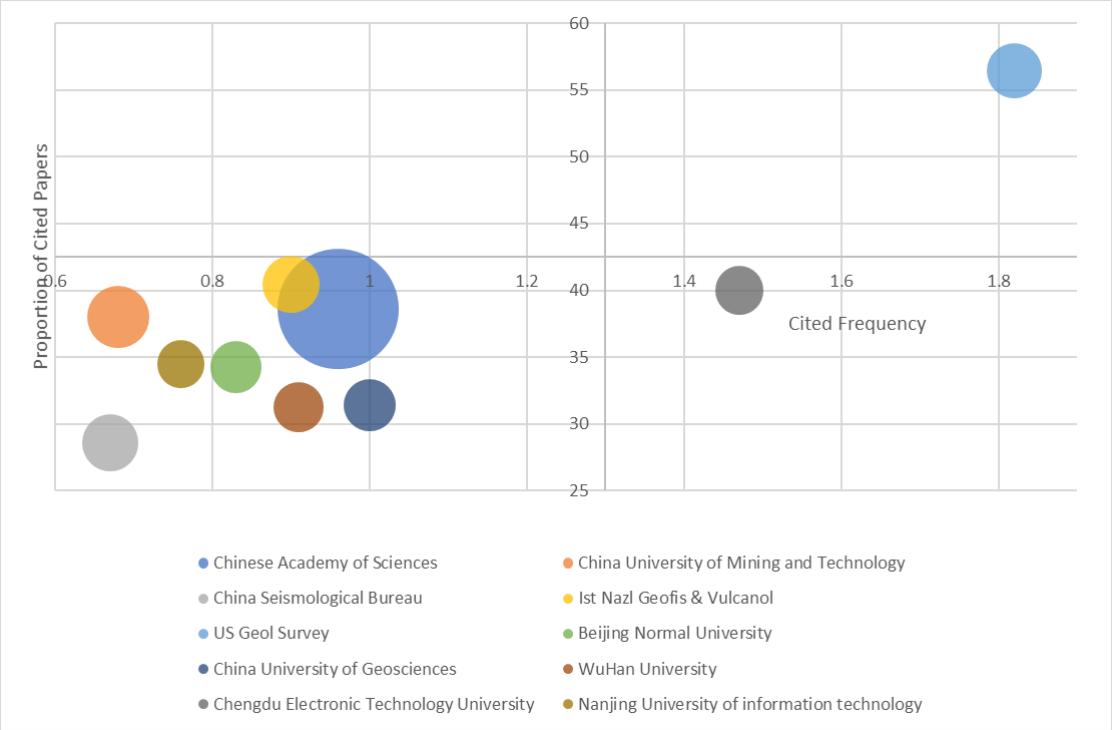

Figure 2 The total number of papers, the cited frequency of the papers and the proportion of cited papers in each institution.

2. Trends of research

2.1 Major subject areas

Based on the WoS platform, disaster prevention research involves a total of 97 subject areas[5], but it is mainly distributed in the following 11 disciplines (in more than 300 papers): Environmental Science, Geoscience Multidisciplinary, Water Resources, Meteorology and Atmospheric Science, Geochemistry and Geophysics, Public Environment and Occupational Health, Engineering Geology, Engineering Environment, Remote Sensing, Geography and Natural Environment Research. The research on disaster prevention in China covers 68 subject areas, but mainly in the following 10 disciplines (with more than 100 papers): Environmental Science, Geoscience Multidisciplinary, Water Resources, Meteorology and Atmospheric Sciences, Engineering Geology, Engineering Environment, Green and Sustainable Technology, Public Environment and Occupational Health, Remote Sensing, and Environmental Research. In the field of disaster prevention in China, there are only a few instances of published research in Geochemistry and Geophysics, as well as in Geography. As shown in Figure 3, most of the papers published on disaster prevention in China mainly involve Environmental Sciences and Geoscience Multidisciplinary, which are more concentrated than other sciences in the world.

[5] Web of Sciences, Disciplinary classification system is a multiple classification system, that is, a paper that may belong to multiple disciplines.

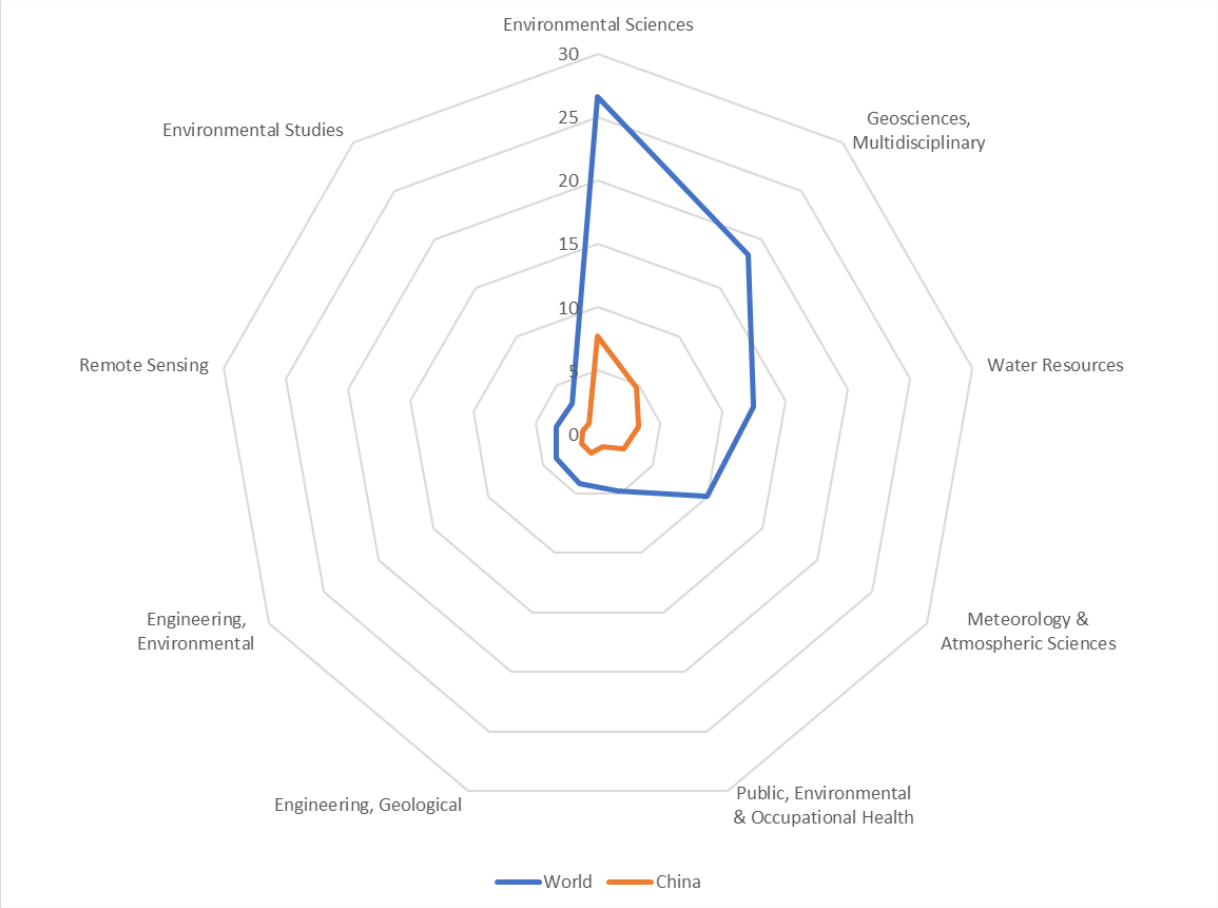

Figure 3 Percentage analysis of papers in major subject areas on disaster prevention research at home and abroad

2.2 Major journals

Published journals represent the study trend. As this study illustrates, the statistics on journals of disaster prevention show that there are 13 journals with more than 30 papers published by Chinese authors, accounting for 78.0% of the total published papers. There are 12 journals with more than 70 papers published by global authors, accounting for 78.0% of the total published papers.

Table 3 Major disaster prevention journals in SCIE database.

Number of published papers	Journals of Chinese authors	Impact factor	Number of published papers	Journals of global authors	Impact factor
93	SUSTAINABILITY	2.592	**276**	INTERNATIONAL JOURNAL	2.468

				OF ENVIRONMENTAL RESEARCH AND PUBLIC HEALTH	
78	INTERNATIONAL JOURNAL OF ENVIRONMENTAL RESEARCH AND PUBLIC HEALTH	2.468	**236**	INTERNATIONAL JOURNAL OF DISASTER RISK REDUCTION	2.568
66	SCIENCE OF THE TOTAL ENVIRONMENT	5.589	**218**	SCIENCE OF THE TOTAL ENVIRONMENT	5.589
59	WATER	2.524	**181**	SUSTAINABILITY	2.592
49	BULLETIN OF ENGINEERING GEOLOGY AND THE ENVIRONMENT	2.138	**165**	NATURAL HAZARDS	2.319
49	REMOTE SENSING	4.118	**151**	WATER	2.524
40	NATURAL HAZARDS	2.319	**128**	REMOTE SENSING	4.118
37	INTERNATIONAL JOURNAL OF DISASTER RISK REDUCTION	2.568	**108**	ENVIRONMENTAL SCIENCE AND POLLUTION RESEARCH	2.914
36	ECOTOXICOLOGY AND ENVIRONMENTAL SAFETY	4.527	**91**	BULLETIN OF ENGINEERING GEOLOGY AND THE ENVIRONMENT	2.138
34	ENVIRONMENTAL SCIENCE AND POLLUTION RESEARCH	2.914	**81**	NATURAL HAZARDS AND EARTH SYSTEM SCIENCES	2.883
32	GEOMATICS NATURAL HAZARDS & RISK	2.332	**75**	CHEMOSPHERE	5.108
30	ENGINEERING GEOLOGY	3.909	**73**	ENVIRONMENT INTERNATIONAL	7.943
30	JOURNAL OF CLEANER PRODUCTION	6.395			

3. Hot topics of research

The research content in this section is based on the method of keyword co-occurrence. The Thomson Data Analyzer software is used to clean the Keywords Plus field of the paper, both by electronic and manual means. Following this process, the VOS viewer software is then used to cluster core topic words of the paper. These words are selected based upon the high-frequency topic words in the particular topic, as discovered in the previously collected data.

Depending on the data set size of the paper, a certain co-occurrence frequency and co-occurrence intensity to cluster keywords is applied. Combined with expert interpretation, each cluster is named and interpreted respectively, and the topics of the journals are identified and analyzed.

The average cited frequency of the core topic words in the analysis results represents the average cited frequency since the time that the paper containing the topic word was published. The average correlation strength represents the closeness between the core topic words contained in the theme concept. The stronger that the topic relevance strength is, the greater the co-occurrence strength between the core topic words is, and as such, the more concentrated the research is. On the other hand, a weaker topic relevance means that the co-occurrence strength is relatively low, and that the research is more scattered.

Keywords Plus is used as an analysis method. After electronic and manual cleaning, 681 keywords with a frequency of more than 10 times are selected from 13,792 keywords. These 681 keywords are used as analysis objects for cluster calculation. By clustering the core topic words with the greatest co-occurrence intensity in these papers, five clusters were obtained. As is shown in Figure 4, the five hot research topics are toxic emissions and environmental pollution disaster, study on the mechanism of earthquake and landslide disaster, model simulation of surface motion, climate change risks and social adaptation, and temperature and extreme weather, respectively.

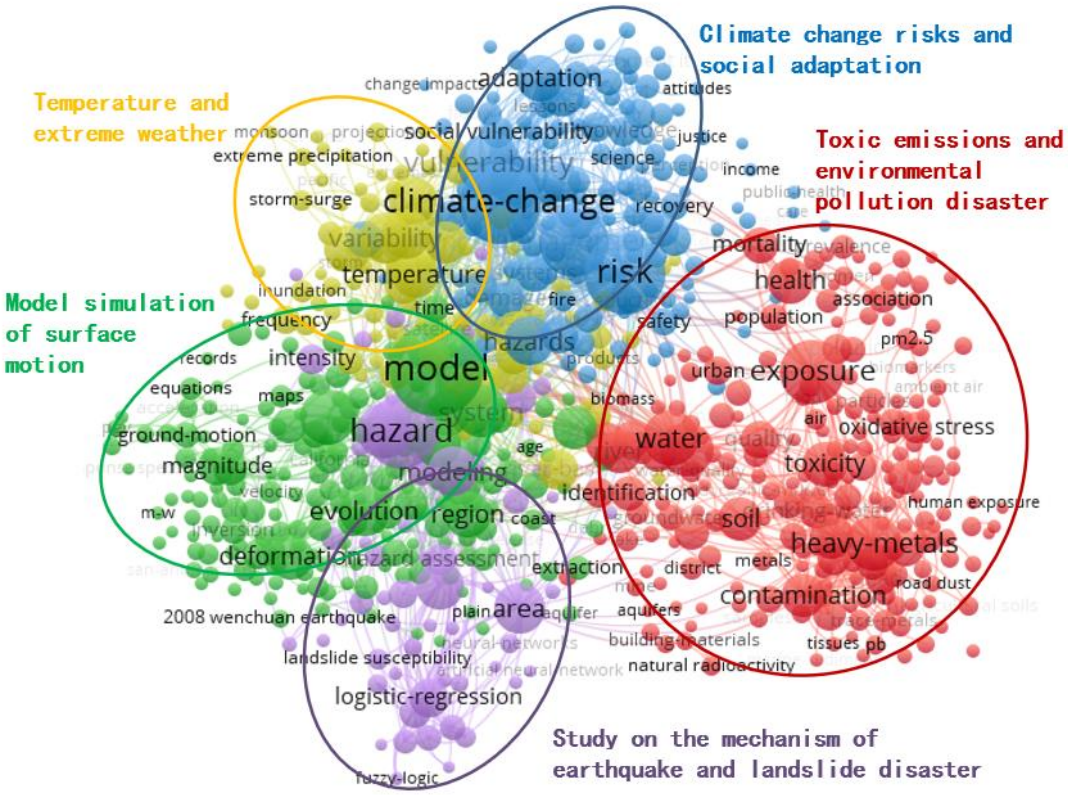

Figure 4 Analysis of research topics in the field of disaster prevention in 2019.

Appendix: Highly cited literature summary

1. Comparison of GIS-based landslide susceptibility models using frequency ratio, logistic regression, and artificial neural network in a tertiary region of Ambon, Indonesia

Journal: Geomorphology

Abstract: This study aims to evaluate landslide causative factors in landslide susceptibility assessments and to compare landslide susceptibility models based on the bivariate frequency ratio (FR), multivariate logistic regression (LR), and artificial neural network (ANN). The majority of landslide occurrences in Ambon, Indonesia is induced by heavy rainfall events where slope failures occur mostly on steep slopes thereby endangering municipality areas at the base of the hills. Eight landslide causative factors were considered in the landslide susceptibility assessments. The causative factors were elevation, slope angle, slope aspect, proximity to stream network, lithology, density of geological boundaries, proximity to faults, and proximity to the road network. The output susceptibility maps were reclassified into five classes ranging from very low to very high susceptibility using Jenks natural breaks method. Twenty percent of all mapped landslides were used as the validation of the susceptibility models. The validity and the accuracy of each model were tested by calculating areas under receiver operating characteristic curves (ROCs), and the

areas under the curve (AUC) for the success rate curves of FR, LR, and ANN were 0.688, 0.687, and 0.734, respectively. The AUC for the prediction rate curve of FR, LR, and ANN were 0.668, 0.667, and 0.717, respectively. All findings of the models show good results with the accuracy of all models being higher than 66%. The ANN method proved to be superior in explaining the relationship of landslide with each factor studied.

2. A comparison of statistical methods and multi-criteria decision making to map flood hazard susceptibility in Northern Iran

Journal: Science of the Total Environment

Abstract: In north of Iran, flood is one of the most important natural hazards that annually inflict great economic damages on humankind infrastructures and natural ecosystems. The Kiasar watershed is known as one of the critical areas in north of Iran, due to numerous floods and waste of water and soil resources, as well as related economic and ecological losses. However, a comprehensive and systematic research to identify flood-prone areas, which may help to establish management and conservation measures, has not been carried out yet. Therefore, this study tested four methods: evidential belief function (EBF), frequency ratio (FR), Technique for Order Preference by Similarity To ideal Solution (TOPSIS) and Vlse Kriterijumsk Optimizacija Kompromisno Resenje (VIKOR) for flood hazard susceptibility mapping (FHSM) in this area. These were combined in two methodological frameworks involving statistical and multi-criteria decision making approaches. The efficiency of statistical and multi-criteria methods in FHSM were compared by using area under receiver operating characteristic (AUROC) curve, seed cell area index and frequency ratio. A database containing flood inventory maps and flood-related conditioning factors was established for this watershed. The flood inventory maps produced included 132 flood conditions, which were randomly classified into two groups, for training (70%) and validation (30%). Analytical hierarchy process (AHP) indicated that slope, distance to stream and land use/land cover are of key importance in flood occurrence in the study catchment. In validation results, the EBF model had a better prediction rate (0.987) and success rate (0.946) than FR, TOPSIS and VIKOR (prediction rate 0.917, 0.888, and 0.810; success rate 0.939, 0.904, and 0.735, respectively). Based on their frequency ratio and seed cell area index values, all models except VIKOR showed acceptable accuracy of classification.

3. Toward Global Soil Moisture Monitoring With Sentinel-1: Harnessing Assets and Overcoming Obstacles

Journal: Ieee Transactions on Geoscience and Remote Sensing

Abstract: Soil moisture is a key environmental variable, important to, e.g., farmers, meteorologists, and disaster management units. Here, we present a method to retrieve surface soil moisture (SSM) from the Sentinel-1 (S-1) satellites, which carry C-band Synthetic Aperture Radar (CSAR) sensors that provide the richest freely available SAR data source so far, unprecedented in accuracy and coverage. Our SSM retrieval

method, adapting well-established change detection algorithms, builds the first globally deployable soil moisture observation data set with 1-km resolution. This paper provides an algorithm formulation to be operated in data cube architectures and high-performance computing environments. It includes the novel dynamic Gaussian upscaling method for spatial upscaling of SAR imagery, harnessing its field-scale information and successfully mitigating effects from the SAR's high signal complexity. Also, a new regression-based approach for estimating the radar slope is defined, coping with Sentinel-1's inhomogeneity in spatial coverage. We employ the S-1 SSM algorithm on a 3-year S-1 data cube over Italy, obtaining a consistent set of model parameters and product masks, unperturbed by coverage discontinuities. An evaluation of therefrom generated S-1 SSM data, involving a 1-km soil water balance model over Umbria, yields high agreement over plains and agricultural areas, with low agreement over forests and strong topography. While positive biases during the growing season are detected, the excellent capability to capture small-scale soil moisture changes as from rainfall or irrigation is evident. The S-1 SSM is currently in preparation toward operational product dissemination in the Copernicus Global Land Service.

4. A Novel Integrated Approach of Relevance Vector Machine Optimized by Imperialist Competitive Algorithm for Spatial Modeling of Shallow Landslides

Journal: Remote Sensing

Abstract: This research aims at proposing a new artificial intelligence approach (namely RVM-ICA) which is based on the Relevance Vector Machine (RVM) and the Imperialist Competitive Algorithm (ICA) optimization for landslide susceptibility modeling. A Geographic Information System (GIS) spatial database was generated from Lang Son city in Lang Son province (Vietnam). This GIS database includes a landslide inventory map and fourteen landslide conditioning factors. The suitability of these factors for landslide susceptibility modeling in the study area was verified by the Information Gain Ratio (IGR) technique. A landslide susceptibility prediction model based on RVM-ICA and the GIS database was established by training and prediction phases. The predictive capability of the new approach was evaluated by calculations of sensitivity, specificity, accuracy, and the area under the Receiver Operating Characteristic curve (AUC). In addition, to assess the applicability of the proposed model, two state-of-the-art soft computing techniques including the support vector machine (SVM) and logistic regression (LR) were used as benchmark methods. The results of this study show that RVM-ICA with AUC = 0.92 achieved a high goodness-of-fit based on both the training and testing datasets. The predictive capability of RVM-ICA outperformed those of SVM with AUC = 0.91 and LR with AUC = 0.87. The experimental results confirm that the newly proposed model is a very promising alternative to assist planners and decision makers in the task of managing landslide prone areas.

5. Landslide susceptibility modelling using GIS-based machine learning techniques

for Chongren County, Jiangxi Province, China

Journal: Science of the Total Environment

Abstract: The preparation of a landslide susceptibility map is considered to be the first step for landslide hazard mitigation and risk assessment. However, these maps are accepted as end products that can be used for land use planning. The main goal of this study is to assess and compare four advanced machine learning techniques, namely the Bayes' net (BN), radical basis function (RBF) classifier, logistic model tree (LMT), and random forest (RF) models, for landslide susceptibility modelling in Chongren County, China. A total of 222 landslide locations were identified in the study area using historical reports, interpretation of aerial photographs, and extensive field surveys. The landslide inventory data was randomly split into two groups with a ratio of 70/30 for training and validation purposes. Fifteen landslide conditioning factors were prepared for landslide susceptibility modelling. The spatial correlation between landslides and conditioning factors was analyzed using the information gain (IG) method. The BN, RBF classifier, LMT, and RF models were constructed using the training dataset. Finally, the receiver operating characteristic (ROC) and statistical measures, including sensitivity, specificity, and accuracy, were employed to validate and compare the predictive capabilities of the models. Out of the tested models, the RF model had the highest sensitivity, specificity, and accuracy values of 0.787, 0.716, and 0.752, respectively, for the training dataset. Overall, the RF model produced an optimized balance for the training and validation datasets in terms of AUC values and statistical measures. The results of this study also demonstrate the benefit of selecting optimal machine learning techniques with proper conditioning selection methods for landslide susceptibility modelling.

6. A novel ensemble approach of bivariate statistical-based logistic model tree classifier for landslide susceptibility assessment

Journal: Geocarto International

Abstract: This study addresses landslide susceptibility mapping (LSM) using a novel ensemble approach of using a bivariate statistical method (weights of evidence [WoE] and evidential belief function [EBF])-based logistic model tree (LMT) classifier. The performance and prediction capability of the ensemble models were assessed using the area under the ROC curve (AUROC), standard error, 95% confidence intervals and significance level P. Model performance analyses indicated that the AUROC values of the WoE–LMT ensemble model using the training and validation data-sets were 86.02 and 85.9%, respectively, whereas those of the EBF–LMT ensemble model were 88.2 and 87.8%, respectively. On the other hand, the AUC curves for the four landslide susceptibility maps indicated that the AUC values of the ensemble models of WoE–LMT (85.11 and 83.98%) and EBF–LMT (86.21 and 85.23%) could improve the performance and prediction accuracy of single WoE (84.23 and 82.46%) and EBF (85.39 and 81.33%) models for the training and validation data-sets.

7. Spatial prediction of landslide susceptibility using data mining-based kernel logistic

regression, naive Bayes and RBFNetwork models for the Long County area (China)
Journal: Bulletin of Engineering Geology and the Environment
Abstract: The main goal of this study is to assess and compare three advanced machine learning techniques, namely, kernel logistic regression (KLR), naïve Bayes (NB), and radial basis function network (RBFNetwork) models for landslide susceptibility modeling in Long County, China. First, a total of 171 landslide locations were identified within the study area using historical reports, aerial photographs, and extensive field surveys. All the landslides were randomly separated into two parts with a ratio of 70/30 for training and validation purposes. Second, 12 landslide conditioning factors were prepared for landslide susceptibility modeling, including slope aspect, slope angle, plan curvature, profile curvature, elevation, distance to faults, distance to rivers, distance to roads, lithology, NDVI (normalized difference vegetation index), land use, and rainfall. Third, the correlations between the conditioning factors and the occurrence of landslides were analyzed using normalized frequency ratios. A multicollinearity analysis of the landslide conditioning factors was carried out using tolerances and variance inflation factor (VIF) methods. Feature selection was performed using the chi-squared statistic with a 10-fold cross-validation technique to assess the predictive capabilities of the landslide conditioning factors. Then, the landslide conditioning factors with null predictive ability were excluded in order to optimize the landslide models. Finally, the trained KLR, NB, and RBFNetwork models were used to construct landslide susceptibility maps. The receiver operating characteristics (ROC) curve, the area under the curve (AUC), and several statistical measures, such as accuracy (ACC), F-measure, mean absolute error (MAE), and root mean squared error (RMSE), were used for the assessment, validation, and comparison of the resulting models in order to choose the best model in this study. The validation results show that all three models exhibit reasonably good performance, and the KLR model exhibits the most stable and best performance. The KLR model, which has a success rate of 0.847 and a prediction rate of 0.749, is a promising technique for landslide susceptibility mapping. Given the outcomes of the study, all three models could be used efficiently for landslide susceptibility analysis.

8. Performance evaluation of the GIS-based data mining techniques of best-first decision tree, random forest, and naive Bayes tree for landslide susceptibility modeling

Journal: Science of the Total Environment
Abstract: The main aim of the present study is to explore and compare three state-of-the art data mining techniques, best-first decision tree, random forest, and naïve Bayes tree, for landslide susceptibility assessment in the Longhai area of China. First, a landslide inventory map with 93 landslide locations was randomly divided, with 70% of the area used for training landslide models and 30% used for the validation process. A spatial database of 14 conditioning factors was constructed under a geographic information system environment. Subsequently, the ReliefF

method was employed to assess the prediction capability of the conditioning factors in landslide models. Multicollinearity of these factors was verified using the variance inflation factor, tolerance, and Pearson's correlation coefficient. Finally, the three resulting models were evaluated and compared using the area under the receiver operating characteristic (AUROC) curve, standard error, 95% confidence interval, accuracy, precision, recall, and F-measure. The random forest model showed the AUROC values (0.869), smallest standard error (0.025), narrowest 95% confidence interval (0.819–0.918), highest accuracy value (0.774), highest precision (0.662), and highest F-measure (0.662) for the training dataset. Thus, the random forest model is a promising technique that could be used for landslide susceptibility mapping.

9. An ensemble prediction of flood susceptibility using multivariate discriminant analysis, classification and regression trees, and support vector machines

Journal: Science of the Total Environment

Abstract: Floods, as a catastrophic phenomenon, have a profound impact on ecosystems and human life. Modeling flood susceptibility in watersheds and reducing the damages caused by flooding is an important component of environmental and water management. The current study employs two new algorithms for the first time in flood susceptibility analysis, namely multivariate discriminant analysis (MDA), and classification and regression trees (CART), incorporated with a widely used algorithm, the support vector machine (SVM), to create a flood susceptibility map using an ensemble modeling approach. A flood susceptibility map was developed using these models along with a flood inventory map and flood conditioning factors (including altitude, slope, aspect, curvature, distance from river, topographic wetness index, drainage density, soil depth, soil hydrological groups, land use, and lithology). The case study area was the Khiyav-Chai watershed in Iran. To ensure a more accurate ensemble model, this study proposed a framework for flood susceptibility assessment where only those models with an accuracy of >80% were permissible for use in ensemble modeling. The relative importance of factors was determined using the Jackknife test. Results indicated that the MDA model had the highest predictive accuracy (89%), followed by the SVM (88%) and CART (0.83%) models. Sensitivity analysis showed that slope percent, drainage density, and distance from river were the most important factors in flood susceptibility mapping. The ensemble modeling approach indicated that residential areas at the outlet of the watershed were very susceptible to flooding, and that these areas should, therefore, be prioritized for the prevention and remediation of floods.

10. Surface ruptures following the 30 October 2016 M-w 6.5 Norcia earthquake, central Italy

Journal: Journal of Maps

Abstract: We present a 1:25,000 scale map of the coseismic surface ruptures following the 30 October 2016 Mw 6.5 Norcia normal-faulting earthquake, central Italy. Detailed rupture mapping is based on almost 11,000 oblique photographs taken

from helicopter flights, that has been verified and integrated with field data (>7000 measurements). Thanks to the common efforts of the Open EMERGEO Working Group (130 people, 25 research institutions and universities from Europe), we were able to document a complex surface faulting pattern with a dominant strike of N135°-160° (SW-dipping) and a subordinate strike of N320°-345° (NEdipping) along about 28 km of the active Mt. Vettore–Mt. Bove fault system. Geometric and kinematic characteristics of the rupture were observed and recorded along closely spaced, parallel or subparallel, overlapping or step-like synthetic and antithetic fault splays of the activated fault systems, comprising a total surface rupture length of approximately 46 km when all ruptures were considered.

11. The 2014 Earthquake Model of the Middle East: ground motion model and uncertainties

Journal: Bulletin of Earthquake Engineering

Abstract: We summarize the main elements of a ground-motion model, as built in three year effort within the Earthquake Model of the Middle East (EMME) project. Together with the earthquake source, the ground-motion models are used for a probabilistic seismic hazard assessment (PSHA) of a region covering eleven countries: Afghanistan, Armenia, Azerbaijan, Cyprus, Georgia, Iran, Jordan, Lebanon, Pakistan, Syria and Turkey. Given the wide variety of ground-motion predictive models, selecting the appropriate ones for modeling the intrinsic epistemic uncertainty can be challenging. In this respect, we provide a strategy for ground-motion model selection based on data-driven testing and sensitivity analysis. Our testing procedure highlights the models of good performance in terms of both data-driven and non-data-driven testing criteria. The former aims at measuring the match between the ground-motion data and the prediction of each model, whereas the latter aims at identification of discrepancies between the models. The selected set of ground models were directly used in the sensitivity analyses that eventually led to decisions on the final logic tree structure. The strategy described in great details hereafter was successfully applied to shallow active crustal regions, and the final logic tree consists of four models (Akkar and C¸ag ˘nan in Bull Seismol Soc Am 100:2978–2995, 2010; Akkar et al. in Bull Earthquake Eng 12(1):359–387, 2014; Chiou and Youngs in Earthq Spectra 24:173–215, 2008; Zhao et al. in Bull Seismol Soc Am 96:898–913, 2006). For other tectonic provinces in the considered region (i.e., subduction), we adopted the predictive models selected within the 2013 Euro-Mediterranean Seismic Hazard Model (Woessner et al. in Bull Earthq Eng 13(12):3553–3596, 2015). Finally, we believe that the framework of selecting and building a regional ground-motion model represents a step forward in ground-motion modeling, particularly for large-scale PSHA models.

12. Urban flood risk mapping using the GARP and QUEST models: A comparative study of machine learning techniques

Journal: Journal of Hydrology

Abstract: Flood risk mapping and modeling is important to prevent urban flood damage. In this study, a flood risk map was produced with limited hydrological and hydraulic data using two state-of-the-art machine learning models: Genetic Algorithm Rule-Set Production (GARP) and Quick Unbiased Efficient Statistical Tree (QUEST). The flood conditioning factors used in modeling were: precipitation, slope, curve number, distance to river, distance to channel, depth to groundwater, land use, and elevation. Based on available reports and field surveys for Sari city (Iran), 113 points were identified as flooded areas (with each flooded zone assigned a value of 1). Different conditioning factors, including urban density, quality of buildings, age of buildings, population density, and socio-economic conditions, were taken into account to analyze flood vulnerability. In addition, the weight of these conditioning factors was determined based on expert knowledge and Fuzzy Analytical Network Process (FANP). An urban flood risk map was then produced using flood hazard and flood vulnerability maps. The area under the receiver-operator characteristic curve (AUC-ROC) and Kappa statistic were applied to evaluate model performance. The results demonstrated that the GARP model (AUC-ROC = 93.5%, Kappa = 0.86) had higher performance accuracy than the QUEST model (AUC-ROC = 89.2%, Kappa = 0.79). The results also indicated that distance to channel, land use, and elevation played major roles in flood hazard determination, whereas population density, quality of buildings, and urban density were the most important factors in terms of vulnerability. These findings demonstrate that machine learning models can help in flood risk mapping, especially in areas where detailed hydraulic and hydrological data are not available.

13. Validation of the CHIRPS satellite rainfall estimates over eastern Africa
Journal: Quarterly Journal of the Royal Meteorological Society

Abstract: Long and temporally consistent rainfall time series are essential in climate analyses and applications. Rainfall data from station observations are inadequate over many parts of the world due to sparse or non-existent observation networks, or limited reporting of gauge observations. As a result, satellite rainfall estimates have been used as an alternative or as a supplement to station observations. However, many satellite-based rainfall products with long time series suffer from coarse spatial and temporal resolutions and inhomogeneities caused by variations in satellite inputs. There are some satellite rainfall products with reasonably consistent time series, but they are often limited to specific geographic areas. The Climate Hazards Group Infrared Precipitation (CHIRP) and CHIRP combined with station observations (CHIRPS) are recently produced satellite-based rainfall products with relatively high spatial and temporal resolutions and quasi-global coverage. In this study, CHIRP and CHIRPS were evaluated over East Africa at daily, dekadal (10-day) and monthly time-scales. The evaluation was done by comparing the satellite products with rain-gauge data from about 1,200 stations. The CHIRP and CHIRPS products were also compared with two similar operational satellite rainfall products: the African Rainfall Climatology version 2 (ARC2) and the Tropical Applications of Meteorology

using Satellite data (TAMSAT). The results show that both CHIRP and CHIRPS products are significantly better than ARC2 with higher skill and low or no bias. These products were also found to be slightly better than the latest version of the TAMSAT product at dekadal and monthly time-scales, while TAMSAT performed better at the daily time-scale. The performance of the different satellite products exhibits high spatial variability with weak performances over coastal and mountainous regions.

14. Assessment of advanced random forest and decision tree algorithms for modeling rainfall-induced landslide susceptibility in the Izu-Oshima Volcanic Island, Japan

Journal: Science of the Total Environment

Abstract: Landslides represent a part of the cascade of geological hazards in a wide range of geo-environments. In this study, we aim to investigate and compare the performance of two state-of-the-art machine learning models, i.e., decision tree (DT) and random forest (RF) approaches to model the massive rainfall-triggered landslide occurrences in the Izu-Oshima Volcanic Island, Japan at a regional scale. At first, a landslide inventory map is prepared consisting of 44 landslide polygons (10,444 pixels) from aerial photo-interpretation and field surveys. To estimate the robustness of the models, we randomly adapted two different samples (S1 and S2), comprising of both positive and negative cells (70% of total landslides - 7293 pixels) for training and remaining (30%-3151 pixels) for validation. Twelve causative factors including altitude, slope angle, slope aspect, plan curvature, total curvature, compound topographic index, stream power index, distance to drainage network, drainage density, distance to geological boundaries, lithology and cumulative rainfall were selected as predictors to implement the landslide susceptibility model. The area under the receiver operating characteristics (ROC) curves (AUC) and other statistical signifiers were used to verify the model accuracies. The result shows that the DT and RF models achieved remarkable predictive performance (AUC > 0.9), producing near accurate susceptibility maps. The overall efficiency of RF (AUC = 0.956) is found significantly higher than the DT (AUC = 0.928) results. Additionally, we noticed that the performance of RF for modeling landslide susceptibility is very robust even though the training and validation samples are altered. Considering the performances, we suggest that both RF and DT models can be used in other similar non-eruption-related landslide studies in the tephra-deposited rich volcanoes, as they are capable of rapidly generating accurate and stable LSM maps for risk mitigation, management practices, and decision-making. Moreover, the RF-based model is promising and enough to be recommended as a method to map regional landslide susceptibility.

15. Copulas-based risk analysis for inter-seasonal combinations of wet and dry conditions under a changing climate

Journal: International Journal of Climatology

Abstract: Abrupt transitions between droughts and floods present greater challenges to water resource management than independent drought or flood events. It is therefore of significant importance to further include drought-flood transitions in the risk analysis of water-related hazards under a changing climate. This study more generally evaluates the risks of combinations of dry and wet conditions between adjacent seasons. First, dry and wet conditions are monitored by the Standardized Precipitation Index (SPI). Then, a copula-based framework is proposed for the deviation of joint return periods of dryness-wetness combinations at different severity levels. In addition, SPI series trend detection is conducted using the Mann-Kendall test to analyse the temporal-spatial changes in dry and wet conditions. Wavelet analysis is applied to investigating correlations of dry and wet conditions with climate variability signals, which may provide predictive signals for dryness-wetness combinations. The results of a case study in the Pearl River basin (PRB), China over the period of 1960–2015 indicate that (1) the flood season (from July to October) tends towards dryness and there are wetting trends in the late autumn and winter; (2) as the joint return period is considered the proxy for the risk of dryness-wetness combination, shorter joint return periods remind a higher risk of suffering from abrupt dryness-wetness transitions in the spring-summer and summer-autumn, as well as the more frequent occurrence of continued dryness/wetness in the autumn-winter and winter-spring; (3) the western and eastern PRB are separately characterized by intensified and reduced risks of the most frequent combinations under a changing climate; and (4) El Niño Southern Oscillation events, the Pacific Decadal Oscillation and sunspot activities have a close association with dry and wet conditions in the PRB. The study provides a supplement for the current risk map and may benefit the early warning and mitigation of water-related hazards.

16. Escalating impacts of climate extremes on critical infrastructures in Europe
Journal: Global Environmental Change-Human and Policy Dimensions

Abstract: Extreme climatic events are likely to become more frequent owing to global warming. This may put additional stress on critical infrastructures with typically long life spans. However, little is known about the risks of multiple climate extremes on critical infrastructures at regional to continental scales. Here we show how singleand multi-hazard damage to energy, transport, industrial, and social critical infrastructures in Europe are likely to develop until the year 2100 under the influence of climate change. We combine a set of high-resolution climate hazard projections, a detailed representation of physical assets in various sectors and their sensitivity to the hazards, and more than 1100 records of losses from climate extremes in a prognostic modelling framework. We find that damages could triple by the 2020s, multiply six-fold by mid-century, and amount to more than 10 timespresentdamageof€3.4billionperyearbytheendofthecenturydueonlytoclimatechange.Damagefrom heatwaves, droughts in southern Europe, and coastal floods shows the most dramatic rise, but the risks of inland flooding,windstorms,andforest fireswillalsoincreaseinEurope,withvaryingdegreesofchangeacrossregions. Economic

losses are highest for the industry, transport, and energy sectors. Future losses will not be incurred equally across Europe. Southern and south-eastern European countries will be most affected and, as a result, will probably require higher costs of adaptation. The findings of this study could aid in prioritizing regional investments to address the unequal burden of impacts and differences in adaptation capacities across Europe.

17. Global review of human-induced earthquakes
Journal: Earth-Science Reviews
Abstract: The Human-induced Earthquake Database, HiQuake, is a comprehensive record of earthquake sequences postulated to be induced by anthropogenic activity. It contains over 700 cases spanning the period 1868-2016. Activities that have been proposed to induce earthquakes include the impoundment of water reservoirs, erecting tall buildings, coastal engineering, quarrying, extraction of groundwater, coal, minerals, gas, oil and geothermal fluids, excavation of tunnels, and adding material to the subsurface by allowing abandoned mines to flood and injecting fluid for waste disposal, enhanced oil recovery, hydrofracturing, gas storage and carbon sequestration. Nuclear explosions induce earthquakes but evidence for chemical explosions doing so is weak. Because it is currently impossible to determine with 100% certainty which earthquakes are induced and which not, HiQuake includes all earthquake sequences proposed on scientific grounds to have been human-induced regardless of credibility. Challenges to constructing HiQuake include under-reporting which is similar to 30% of M similar to 4 events, 60% of M similar to 3 events and similar to 90% of M similar to 2 events. The amount of stress released in an induced earthquake is not necessarily the same as the anthropogenic stress added because pre-existing tectonic stress may also be released. Thus earthquakes disproportionately large compared with the associated industrial activity may be induced. Knowledge of the magnitude of the largest earthquake that might be induced by a project, M,,, is important for hazard reduction. Observed M-MAX correlates positively with the scale of associated industrial projects, fluid injection pressure and rate, and the yield of nuclear devices. It correlates negatively with calculated inducing stress change, likely because the latter correlates inversely with project scale. The largest earthquake reported to date to be induced by fluid injection is the 2016 M 5.8 Pawnee, Oklahoma earthquake, by water-reservoir impoundment the 2008 M similar to 8 Wenchuan, People's Republic of China, earthquake, and by mass removal the 1976 M 7.3 Gazli, Uzbekistan earthquake. The minimum amount of anthropogenic stress needed to induce an earthquake is an unsound concept since earthquakes occur in the absence of industrial activity. The minimum amount of stress observed to modulate earthquake activity is a few hundredths of a megapascal and possibly as little as a few thousandths, equivalent to a few tens of centimeters of water-table depth. Faults near to failure are pervasive in the continental crust and induced earthquakes may thus occur essentially anywhere. In intraplate regions neither infrastructure nor populations may be prepared for earthquakes. Human-induced earthquakes that cause nuisance are rare, but in some cases may be a significant problem, e.g., in the hydrocarbon-producing areas of

Oklahoma, USA. As the size of projects and density of populations increase, the potential nuisance of induced earthquakes is also increasing and effective management strategies are needed.

18. Evaluation of Different Machine Learning Methods and Deep-Learning Convolutional Neural Networks for Landslide Detection

Journal: Remote Sensing

Abstract: There is a growing demand for detailed and accurate landslide maps and inventories around the globe, but particularly in hazard-prone regions such as the Himalayas. Most standard mapping methods require expert knowledge, supervision and fieldwork. In this study, we use optical data from the Rapid Eye satellite and topographic factors to analyze the potential of machine learning methods, i.e., artificial neural network (ANN), support vector machines (SVM) and random forest (RF), and different deep-learning convolution neural networks (CNNs) for landslide detection. We use two training zones and one test zone to independently evaluate the performance of different methods in the highly landslide-prone Rasuwa district in Nepal. Twenty different maps are created using ANN, SVM and RF and different CNN instantiations and are compared against the results of extensive fieldwork through a mean intersection-over-union (mIOU) and other common metrics. This accuracy assessment yields the best result of 78.26% mIOU for a small window size CNN, which uses spectral information only. The additional information from a 5 m digital elevation model helps to discriminate between human settlements and landslides but does not improve the overall classification accuracy. CNNs do not automatically outperform ANN, SVM and RF, although this is sometimes claimed. Rather, the performance of CNNs strongly depends on their design, i.e., layer depth, input window sizes and training strategies. Here, we conclude that the CNN method is still in its infancy as most researchers will either use predefined parameters in solutions like Google TensorFlow or will apply different settings in a trial-and-error manner. Nevertheless, deep-learning can improve landslide mapping in the future if the effects of the different designs are better understood, enough training samples exist, and the effects of augmentation strategies to artificially increase the number of existing samples are better understood.

19. Climate change and the global pattern of moraine-dammed glacial lake outburst floods

Journal: Cryosphere

Abstract: Despite recent research identifying a clear anthropogenic impact on glacier recession, the effect of recent climate change on glacier-related hazards is at present unclear. Here we present the first global spatio-temporal assessment of glacial lake outburst floods (GLOFs) focusing explicitly on lake drainage following moraine dam failure. These floods occur as mountain glaciers recede and downwaste. GLOFs can have an enormous impact on downstream communities and infrastructure. Our assessment ofGLOFs associated with the rapid drainage of moraine-dammed lakes

provides insights into the historical trends of GLOFs and their distributions under current and future global climate change. We observe a clear global increase in GLOF frequency and their regularity around 1930, which likely represents a lagged response to post-Little Ice Age warming. Notably, we also show that GLOF frequency and regularity – rather unexpectedly – have declined in recent decades even during a time of rapid glacier recession. Although previous studies have suggested that GLOFs will increase in response to climate warming and glacier recession, our global results demonstrate that this has not yet clearly happened. From an assessment of the timing of climate forcing, lag times in glacier recession, lake formation and moraine-dam failure, we predict increased GLOF frequencies during the next decades and into the 22nd century.

20. Landslide spatial modelling using novel bivariate statistical based Naive Bayes, RBF Classifier, and RBF Network machine learning algorithms

Journal: Science of the Total Environment

Abstract: Landslides are major hazards for human activities often causing great damage to human lives and infrastructure. Therefore, the main aim of the present study is to evaluate and compare three machine learning algorithms (MLAs) including Naive Bayes (NB), radial basis function (RBF) Classifier, and RBF Network for landslide susceptibility mapping (LSM) at Longhai area in China. A total of 14 landslide conditioning factors were obtained from various data sources, then the frequency ratio (FR) and support vector machine (SVM) methods were used for the correlation and selection the most important factors for modelling process, respectively. Subsequently, the resulting three models were validated and compared using some statistical metrics including area under the receiver operating characteristics (AUROC) curve, and Friedman and Wilcoxon signed-rank tests The results indicated that the RBF Classifier model had the highest goodness-of-fit and performance based on the training and validation datasets. The results concluded that the RBF Classifier model outperformed and outclassed (AUROC = 0.881), the NB (AUROC = 0.872) and the RBF Network (AUROC = 0.854) models. The obtained results pointed out that the RBF Classifier model is a promising method for spatial prediction of landslide over the world. (C) 2019 Published by Elsevier B.V.

21. Landslide susceptibility mapping using J48 Decision Tree with AdaBoost, Bagging and Rotation Forest ensembles in the Guangchang area (China)

Journal: Catena

Abstract: Landslides are a manifestation of slope instability causing different kinds of damage affecting life and property. Therefore, high-performance-based landslide prediction models are useful to government institutions for developing strategies for landslide hazard prevention and mitigation. Development of data mining based algorithms shows that high-performance models can be obtained using ensemble frameworks. The primary objective of this study is to investigate and compare the use of current state-of-the-art ensemble techniques, such as AdaBoost, Bagging, and

Rotation Forest, for landslide susceptibility assessment with the base classifier of J48 Decision Tree (JDT). The Guangchang district (Jiangxi province, China) was selected as the case study. Firstly, a landslide inventory map with 237 landslide locations was constructed; the landslide locations were then randomly divided into a ratio of 70/30 for the training and validating models. Secondly, fifteen landslide conditioning factors were prepared, such as slope, aspect, altitude, topographic wetness index (TWI), stream power index (SPI), sediment transport index (STI), plan curvature, profile curvature, lithology, distance to faults, distance to rivers, distance to roads, land use, normalized difference vegetation index (NDVI), and rainfall. Relief-F with the 10-fold cross-validation method was applied to quantify the predictive ability of the conditioning factors and for feature selection. Using the JDT and its three ensemble techniques, a total of four landslide susceptibility models were constructed. Finally, the overall performance of the resulting models was assessed and compared using area under the receiver operating characteristic (ROC) curve (AUC) and statistical indexes. The result showed that all landslide models have high performance (AUC > 0.8). However, the JDT with the Rotation Forest model presents the highest prediction capability (AUC = 0.855), followed by the JDT with the AdaBoost (0.850), the Bagging (0.839), and the JDT (0.814), respectively. Therefore, the result demonstrates that the JDT with Rotation Forest is the best optimized model in this study and it can be considered as a promising method for landslide susceptibility mapping in similar cases for better accuracy.

22. Flood susceptibility assessment in Hengfeng area coupling adaptive neuro-fuzzy inference system with genetic algorithm and differential evolution

Journal: Science of the Total Environment

Abstract: Floods are among Earth's most common natural hazards, and they cause major economic losses and seriously affect peoples' lives and health. This paper addresses the development of a flood susceptibility assessment that uses intelligent techniques and GIS. An adaptive neuro-fuzzy inference system (ANFIS) was coupled with a genetic algorithm and differential evolution for flood spatial modelling. The model considers thirteen hydrologic, morphologic and lithologic parameters for the flood susceptibility assessment, and Hengfeng County in China was chosen for the application of the model due to data availability and the 195 total flood events. The flood locations were randomly divided into two subsets, namely, training (70% of the total) and testing (30%). The Step-wise Weight Assessment Ratio Analysis (SWARA) approach was used to assess the relation between the floods and influencing parameters. Subsequently, two data mining techniques were combined with the ANFIS model, including the ANFIS-Genetic Algorithm and the ANFIS-Differential Evolution, to be used for flood spatial modelling and zonation. The flood susceptibility maps were produced, and their robustness was checked using the Receiver Operating Characteristic (ROC) curve. The results showed that the area under the curve (AUC) for all models was >0.80. The highest AUC value was for the ANFIS-DE model (0.852), followed by ANFIS-GA (0.849). According to the RMSE

and MSE methods, the ANFIS-DE hybrid model is more suitable for flood susceptibility mapping in the study area. The proposed method is adaptable and can easily be applied in other sites for flood management and prevention.

23. Landslide susceptibility assessment at the Wuning area, China: a comparison between multi-criteria decision making, bivariate statistical and machine learning methods

Journal: Natural Hazards

Abstract: The aim of this research is to investigate multi-criteria decision making [spatial multi-criteria evaluation (SMCE)], bivariate statistical methods [frequency ratio (FR), index of entropy (IOE), weighted linear combination (WLC)] and machine learning [support vector machine (SVM)] models for estimating landslide susceptibility at the Wuning area, China. A total of 445 landslides were randomly classified into 70% (311 landslides) and 30% (134 landslides) to train and validate landslide models, respectively. Fourteen landslide conditioning factors including slope angle, slope aspect, altitude, topographic wetness index, stream power index, sediment transport index, soil, lithology, NDVI, land use, rainfall, distance to road, distance to river and distance to fault were then studied for landslide susceptibility assessment. Performances of five studied models were evaluated using area under the ROC curve (AUROC) for training (success rate curve) and validation (prediction rate curve) datasets, statistical-based measures and tests. Results indicated that the area under the success rate curve for the FR, IOE, WLC, SVM and SMCE models was 88.32%, 82.58%, 78.91%, 85.47% and 89.96%, respectively, demonstrating that SMCE could provide the higher accuracy. The prediction capability findings revealed that the SMCE model (AUC=86.81%) was also the highest approach among the five studied models, followed by the FR (AUC=84.53%), the SVM (AUC=81.24%), the IOE (AUC=79.67%) and WLC (73.92%) methods. The landslide susceptibility maps derived from the above five models are reasonably accurate and could be used to perform elementary land use planning for hazard extenuation.

24. Application of fuzzy weight of evidence and data mining techniques in construction of flood susceptibility map of Poyang County

Journal: Science of the Total Environment

Abstract: In China, floods are considered as the most frequent natural disaster responsible for severe economic losses and serious damages recorded in agriculture and urban infrastructure. Based on the international experience prevention of flood events may not be completely possible, however identifying susceptible and vulnerable areas through prediction models is considered as a more visible task with flood susceptibility mapping being an essential tool for flood mitigation strategies and disaster preparedness. In this context, the present study proposes a novel approach to construct a flood susceptibility map in the Poyang County, JiangXi Province, China by implementing fuzzy weight of evidence (fuzzy-WofE) and data mining methods. The novelty of the presented approach is the usage of fuzzy-WofE that had a twofold

purpose. Firstly, to create an initial flood susceptibility map in order to identify non-flood areas and secondly to weight the importance of flood related variables which influence flooding. Logistic Regression (LR), Random Forest (RF) and Support Vector Machines (SVM) were implemented considering eleven flood related variables, namely: lithology, soil cover, elevation, slope angle, aspect, topographic wetness index, stream power index, sediment transport index, plan curvature, profile curvature and distance from river network. The efficiency of this new approach was evaluated using area under curve (AUC) which measured the prediction and success rates. According to the outcomes of the performed analysis, the fuzzy WofE-SVM model was the model with the highest predictive performance (AUC value, 0.9865) which also appeared to be statistical significant different from the other predictive models, fuzzy WofERF (AUC value, 0.9756) and fuzzy WofE-LR (AUC value, 0.9652). The proposed methodology and the produced flood susceptibility map could assist researchers and local governments in flood mitigation strategies.

25. A natural language processing and geospatial clustering framework for harvesting local place names from geotagged housing advertisements

Journal: International Journal of Geographical Information Science

Abstract: Local place names are frequently used by residents living in a geographic region. Such place names may not be recorded in existing gazetteers, due to their vernacular nature, relative insignificance to a gazetteer covering a large area (e.g. the entire world), recent establishment (e.g. the name of a newly-opened shopping center) or other reasons. While not always recorded, local place names play important roles in many applications, from supporting public participation in urban planning to locating victims in disaster response. In this paper, we propose a computational framework for harvesting local place names from geotagged housing advertisements. We make use of those advertisements posted on local-oriented websites, such as Craigslist, where local place names are often mentioned. The proposed framework consists of two stages: natural language processing (NLP) and geospatial clustering. The NLP stage examines the textual content of housing advertisements and extracts place name candidates. The geospatial stage focuses on the coordinates associated with the extracted place name candidates and performs multiscale geospatial clustering to filter out the non-place names. We evaluate our framework by comparing its performance with those of six baselines. We also compare our result with four existing gazetteers to demonstrate the not-yet-recorded local place names discovered by our framework.

26. Hybrid artificial intelligence models based on a neuro-fuzzy system and metaheuristic optimization algorithms for spatial prediction of wildfire probability

Journal: Agricultural and Forest Meteorology

Abstract：This study provides a new comparative analysis of four hybrid artificial intelligence models for the spatially explicit prediction of wildfire probabilities. Each model consists of an adaptive neuro-fuzzy inference system (ANFIS) combined with

a metaheuristic optimization algorithm, i.e., genetic algorithm (GA), particle swarm optimization (PSO), shuffled frog leaping algorithm (SFLA), and imperialist competitive algorithm (ICA). A spatial database was constructed based on 159 fire events from the Hyrcanian ecoregion (Iran) for which a suite of predictor variables was derived. Each predictor variable was discretized into classes. The step-wise weight assessment ratio analysis (SWARA) procedure was used to assign weights to each class of each predictor variable. Weights indicate the strength of the spatial relationship between each class and fire occurrence and were used for training the hybrid models. The hybrid models were validated using several performance metrics and compared to the single ANFIS model. Although the single ANFIS model outperformed the hybrid models in the training phase, its accuracy decreased considerably in the validation phase. All hybrid models performed well for both training and validation datasets, but the ANFIS-ICA hybrid showed superior predictive performance of spatially explicit wildfire prediction and mapping for the dataset. The results clearly demonstrate the ability of the optimization algorithms to overcome the over-fitting problem of the single ANFIS model at the learning stage of the fire pattern. This study contributes to the suite of research that seeks to obtain reliable estimates of relative likelihoods of natural hazards.

27. Assessment of the effects of training data selection on the landslide susceptibility mapping: a comparison between support vector machine (SVM), logistic regression (LR) and artificial neural networks (ANN)

Journal: Geomatics Natural Hazards & Risk

Abstract: Landslide is a natural hazard that results in many economic damages and human losses every year. Numerous researchers have studied landslide susceptibility mapping (LSM), each attempting to improve the accuracy of the final outputs. However, few studies have been published on the training data selection effects on the LSM. Thus, this study assesses the training landslides random selection effects on support vector machine (SVM) accuracy, logistic regression (LR) and artificial neural networks (ANN) models for LSM in a catchment at the Dodangeh watershed, Mazandaran province, Iran. A 160 landslide locations inventory was collected by Geological Survey of Iran for this investigation. Different methods were implemented to define the landslide locations, such as inventory reports, satellite images and field survey. Moreover, 14 landslide conditioning factors were considered in the analysis of landslide susceptibility. These factors include curvature, plan curvature, profile curvature, altitude, slope angle, slope aspect, distance to faults, distance to stream, topographic wetness index, stream power index, terrain roughness index, sediment transport index, lithology and land use. The results show that the random landslide training data selection affected the parameter estimations of the SVM, LR and ANN algorithms. The results also show that the training samples selection had an effect on the accuracy of the susceptibility model because landslide conditioning factors vary according to the geographic locations in the study area. The LR model was found to be less sensitive than the SVM and ANN models to the training samples selection.

Validation results showed that SVM and LR models outperformed the ANN model for all scenarios. The average overall accuracy of LR, SVM and ANN models are 81.42%, 79.82% and 70.2%, respectively.

28. A comparative assessment of decision trees algorithms for flash flood susceptibility modeling at Haraz watershed, northern Iran

Journal: Science of the Total Environment

Abstract: Floods are one of the most damaging natural hazards causing huge loss of property, infrastructure and lives. Prediction of occurrence of flash flood locations is very difficult due to sudden change in climatic condition and manmade factors. However, prior identification of flood susceptible areas can be done with the help of machine learning techniques for proper timely management of flood hazards. In this study, we tested four decision trees based machine learning models namely Logistic Model Trees (LMT), Reduced Error Pruning Trees (REPT), Naïve Bayes Trees (NBT), and Alternating Decision Trees (ADT) for flash flood susceptibility mapping at the Haraz Watershed in the northern part of Iran. For this, a spatial database was constructed with 201 present and past flood locations and eleven flood-influencing factors namely ground slope, altitude, curvature, Stream Power Index (SPI), Topographic Wetness Index (TWI), land use, rainfall, river density, distance from river, lithology, and Normalized Difference Vegetation Index (NDVI). Statistical evaluation measures, the Receiver Operating Characteristic (ROC) curve, and Freidman and Wilcoxon signed-rank tests were used to validate and compare the prediction capability of the models. Results show that the ADT model has the highest prediction capability for flash flood susceptibility assessment, followed by the NBT, the LMT, and the REPT, respectively. These techniques have proven successful in quickly determining flood susceptible areas.

29. Landslide susceptibility mapping using random forest and boosted tree models in Pyeong-Chang, Korea

Journal: Geocarto International

Abstract: Landslides susceptibility maps were constructed in the Pyeong-Chang area, Korea, using the Random Forest and Boosted Tree models. Landslide locations were randomly selected in a 50/50 ratio for training and validation of the models. Seventeen landslide-related factors were extracted and constructed in a spatial database. The relationships between the observed landslide locations and these factors were identified by using the two models. The models were used to generate a landslide susceptibility map and the importance of the factors was calculated. Finally, the landslide susceptibility maps were validated. Finally, landslide susceptibility maps were generated. For the Random Forest model, the validation accuracy in regression and classification algorithms showed 79.34 and 79.18%, respectively, and for the Boosted Tree model, these were 84.87 and 85.98%, respectively. The two models showed satisfactory accuracies, and the Boosted Tree model showed better results than the Random Forest model.

30. Shallow Fault Rupture of the Milun Fault in the 2018 M-w 6.4 Hualien Earthquake: A High-Resolution Approach from Optical Correlation of Pleiades Satellite Imagery

Journal: Seismological Research Letters

Abstract: We use high-resolution Pléiades optical satellite imagery to study the distribution and magnitude of fault slip along the Milun fault surface rupture, which broke during the 2018 Hualien earthquake (Mw 6.4) in eastern Taiwan. Correlation of pre- and postearthquake stereo Pléiades images reveals detailed 3D surface displacements along the 8-km-long Milun fault, with maximum ∼1 m left-lateral offsets across the fault. Along the northern section of the Milun fault, our correlation results indicate a localized deformation zone, with offset values slightly larger than the maximum offsets reported in the field (∼77 cm). To the south, the left-lateral offsets become increasingly distributed, producing arctangent shapes in displacement profiles crossing the fault. In places, the deformation zone reaches widths of 200+m and can be explained by a shallow east-dipping fault rupture extending from 2 to 3 km depth to 70–120 m below the surface. A very shallow coseismic rupture on the Milun fault is consistent with a shallow locking depth interpreted from previous geodetic analyses from the interseismic period. Despite a few highly discontinuous and irregular surface ruptures reported along the southern section of the fault, our results suggest the main fault slip (up to 1 m) stopped at very shallow depths below the surface, in which ∼60% of the deformation may be accommodated as off-fault deformation (OFD). In this upper ∼100 m of the crust, OFD may be promoted by a significant change in material strength, as the fault crosses from bedrock and/or consolidated sediments into weaker, water-rich, poorly consolidated alluvial sediments.

31. Monitoring hydrological drought using long-term satellite-based precipitation data

Journal: Science of the Total Environment

Abstract: Long-term (over 30a) satellite-based quantitative rainfall estimate (SRE) products provide an ideal data source for hydrological drought monitoring. This study mainly explores the suitability of the two long-term SREs, the Precipitation Estimation from Remotely Sensed Information using Artificial Neural Networks-Climate Data Record (PERSIANN-CDR) and the Climate Hazards Group (CHG) Infrared Precipitation with Stations (CHIRPS), for hydrological drought monitoring. A hydrological drought index called the standardized streamflow index (SSI) was used as an example and the Grid-based Xinanjiang (GXAJ) hydrological model was used for streamflow generation of the SREs. A middle size basin in the humid region of south China was selected as case study. The obtained results show that both SREs present acceptable performances for hydrological modeling, and CHIRPS outperformed PERSIANN-CDR. SSIs calculated by the SRE simulations generally fit well with the trend of observation-based on SSI but apparent deviations in drought intensity were also found. In contrast to hydrological modeling,

performance of the SRE-based SSI showed almost no change after model recalibration. Both SREs generally present acceptable classification accuracy but tended to underestimate the levels of drought types. Both SREs accurately captured the beginning, end, and duration of this drought event; however, several deviations were found in severity and intensity estimation of the drought event. In general, both SREs are suitable for hydrological drought monitoring. Although the CHIRPS generally presented better performance, the PERSIANN-CDR is still adequate for hydrological drought monitoring.

32. Assessment of Geohazards and Preventative Countermeasures Using AHP Incorporated with GIS in Lanzhou, China

Journal: Sustainability

Abstract: This research investigates geohazards and preventative countermeasures for Lanzhou City, China. To investigate the factors related to the development of geohazards in Lanzhou, the regional geological conditions around Lanzhou were investigated. The geomorphology of the region is comprised of a loess landform underlying quaternary loess deposits. A large number of faults induced by strong neotectonic movements are present in the area. Therefore, earthquakes frequently occur around Lanzhou. Earthquakes cause numerous rock falls and landslides, with landslide masses found scattered on the upper middle level of the area's mountains. When intense rainfall occurs, a lot of loose deposits are brought together along steep gullies, forming debris flows; hence, a disaster chain of earthquake–landslide–debris flow is formed. To evaluate the georisks around Lanzhou, the Analytic Hierarchy Process (AHP) was employed to assess geohazards. The spatial distribution of the evaluated georisk levels was mapped using a Geographic Information System (GIS). Based on the assessed results, about 55% of the urban area and 44% of Gaolan County have high or very high-risk levels. The ratio of relatively high disaster risk levels is up to 31% of the total area. To mitigate these geohazards, both strategic decision making and technical countermeasures should be implemented.

33. On the Use of Unmanned Aerial Systems for Environmental Monitoring

Journal: Remote Sensing

Abstract: Environmental monitoring plays a central role in diagnosing climate and management impacts on natural and agricultural systems; enhancing the understanding of hydrological processes; optimizing the allocation and distribution of water resources; and assessing, forecasting, and even preventing natural disasters. Nowadays, most monitoring and data collection systems are based upon a combination of ground-based measurements, manned airborne sensors, and satellite observations. These data are utilized in describing both small- and large-scale processes, but have spatiotemporal constraints inherent to each respective collection system. Bridging the unique spatial and temporal divides that limit current monitoring platforms is key to improving our understanding of environmental systems. In this context, Unmanned Aerial Systems (UAS) have considerable potential to radically

improve environmental monitoring. UAS-mounted sensors offer an extraordinary opportunity to bridge the existing gap between field observations and traditional air- and space-borne remote sensing, by providing high spatial detail over relatively large areas in a cost-effective way and an entirely new capacity for enhanced temporal retrieval. As well as showcasing recent advances in the field, there is also a need to identify and understand the potential limitations of UAS technology. For these platforms to reach their monitoring potential, a wide spectrum of unresolved issues and application-specific challenges require focused community attention. Indeed, to leverage the full potential of UAS-based approaches, sensing technologies, measurement protocols, postprocessing techniques, retrieval algorithms, and evaluation techniques need to be harmonized. The aim of this paper is to provide an overview of the existing research and applications of UAS in natural and agricultural ecosystem monitoring in order to identify future directions, applications, developments, and challenges.

34. Evaluation of the Global Precipitation Measurement (GPM) Satellite Rainfall Products over the Lower Colorado River Basin, Texas

Journal: Journal of the American Water Resources Association

Abstract: Quality of precipitation products from the Integrated Multi-satellitE Retrievals for Global Precipitation Measurement mission (IMERG) was evaluated over the Lower Colorado River Basin of Texas. Observations of several rainfall events of a wide range of magnitudes during May 2015 by a very dense network of 241 rain gauges over the basin were used as a reference. The impact of temporal and spatial downscaling of different satellite products (near/post-real-time) on their accuracy was studied. Generally, all IMERG products perform better when the temporal and spatial resolutions are downscaled. The Final product shows relatively better performance compared to the near-real-time products in terms of basic performance measures; however, regarding rainfall detection, all products show nearly similar performance. When considering rainfall detection, IMERG adequately captures the precipitation events; however, in terms of spatial patterns and accuracy, more improvements are needed. IMERG products analysis results may help developers gain insight into the regional performance of the product, improve the product algorithms, and provide information to end users on the products' suitability for potential hydrometeorological applications. Overall, the IMERG products, even the uncalibrated product at its finest resolution, showed reasonable performance indicating their great potential for applications such as water resources management, prevention of natural disasters, and flood forecasting.

35. A novel hybrid intelligent model of support vector machines and the MultiBoost ensemble for landslide susceptibility modeling

Journal: Bulletin of Engineering Geology and the Environment

Abstract: The main aim of this study is to propose a novel hybrid intelligent model named MBSVM which is an integration of the MultiBoost ensemble and a support

vector machine (SVM) for modeling of susceptibility of landslides in the Uttarakhand State, Northern India. Firstly, a geospatial database for the study area was prepared, which includes 391 historical landslides and 16 landslide-affecting factors. Then, the sensitivity of different combinations of these factors for modeling was validated using the forward elimination technique. The MBSVM landslide model was built using the datasets generated from the best selected factors and validated utilizing the area under the receiver operating characteristic (ROC) curve (AUC), statistical indexes, and the Wilcoxon signed-rank test. Results show that this novel hybrid model has good performance both in terms of goodness of fit with the training dataset (AUC=0.972) and the capability to predict landslides with the testing dataset (AUC=0.966). The efficiency of the proposed model was then validated by comparison with logistic regression (LR), a single SVM, and another hybrid model of the AdaBoost ensemble and an SVM (ABSVM). Comparison results show that the MBSVM outperforms the LR, single SVM, and hybrid ABSVM models. Thus, the proposed model is a promising and good alternative tool for landslide hazard assessment in landslide-prone areas.

36. A novel hybrid approach of landslide susceptibility modelling using rotation forest ensemble and different base classifiers

Journal: GEOCARTO INTERNATIONAL

Abstract: In the present study, Rotation Forest ensemble was integrated with different base classifiers to develop different hybrid models namely Rotation Forest based Support Vector Machines (RFSVM), Rotation Forest based Artificial Neural Networks (RFANN), Rotation Forest based Decision Trees (RFDT), and Rotation Forest based Naïve Bayes (RFNB) for landslide susceptibility modelling. The validity of these models was evaluated using statistical methods such as Root Mean Square Error (RMSE), Kappa index, accuracy, and the area under the success rate and predictive rate curves (AUC). Part of the landslide prone area of Pithoragarh district, Uttarakhand, Himalaya, India was selected as the study area. Results indicate that the RFDT is the best model showing the highest predictive capability (AUC=0.741) in comparison to RFANN (AUC=0.710), RFSVM (AUC=0.701), and RFNB (AUC=0.640) models. The present study would be helpful in the selection of best model for landslide susceptibility mapping.

37. A hybrid machine learning ensemble approach based on a Radial Basis Function neural network and Rotation Forest for landslide susceptibility modeling: A case study in the Himalayan area, India

Journal: International Journal of SEDIMENT RESEARCH

Abstract: In this paper, a hybrid machine learning ensemble approach namely the Rotation Forest based Radial Basis Function (RFRBF) neural network is proposed for spatial prediction of land slides in part of the Himalayan area (India). The proposed approach is an integration of the Radial Basis Function(RBF)neural network classifier and Rotation Forest ensemble, which are state-of-the art machine learning algorithms

for classification problems. For this purpose, a spatial data base of the study area was established that consists of 930 land slide location sand fifteen influencing parameters(slope angle, road density, curvature, land use, distance to road, plan curvature, lineament density, distance to lineaments, rainfall, distance to river, profile curvature, elevation, slope aspect, river density, and soil type).Using the database, training and validation datasets were generated for constructing and validating the model. Performance of the model was assessed using the Receiver Operating Characteristic (ROC) curve, area under the ROC curve (AUC), statistical analysis methods, and the Chi square test. In addition, Logistic Regression (LR), Multi-layer Perceptron Neural Networks (MLP Neural Nets), Naïve Bayes (NB), and the hybrid model of Rotation Forest and Decision Trees (RFDT) were selected for comparison. The results show that the proposed RFRBF model has the highest prediction capability in comparison to the other models (LR,MLP Neural Nets, NB, and RFDT); therefore, the proposed RFRBF model is promising and should be used as an alternative technique for land slide susceptibility modeling.

38．Prediction of the landslide susceptibility: Which algorithm, which precision?
Journal: Catena
Abstract: Coupling machine learning algorithms with spatial analytical techniques for landslide susceptibility modeling is a worth considering issue. So, the current research intend to present the first comprehensive comparison among the performances of ten advanced machine learning techniques (MLTs) including artificial neural networks (ANNs), boosted regression tree (BRT), classification and regression trees (CART), generalized linear model (GLM), generalized additive model (GAM), multivariate adaptive regression splines (MARS), naïve Bayes (NB), quadratic discriminant analysis (QDA), random forest (RF), and support vector machines (SVM) for modeling landslide susceptibility and evaluating the importance of variables in GIS and R open source software. This study was carried out in the Ghaemshahr Region, Iran. The performance of MLTs has been evaluated using the area under ROC curve (AUC-ROC) approach. The results showed that AUC values for ten MLTs vary from 62.4 to 83.7%. It has been found that the RF (AUC =83.7%) and BRT (AUC =80.7%) have the best performances comparison to other MLTs.

39. Typhoon triggered operation tunnel debris flow disaster in coastal areas of SE China
Journal: Environ Monit Assess
Abstract: Typhoons have inflicted significant damage and loss of life to China, a large number of typhoon-rainstorm-debris flow-tunnel accidents occur in the southeastern coastal areas each year. Considering the disaster prevention and mitigation decision-making of disaster accidents in coastal areas and the reduction of regional economic losses, this Express Letter presents some typical accident scenes and rescue measures in recent years and analyses the hazard mechanism from three aspects. On this basis, we propose some suggestions such as the monitoring and early-warning

system, which can provide a few references for reducing disaster losses and improving disaster treatments.

40. The size, distribution, and mobility of landslides caused by the 2015 M(w)7.8 Gorkha earthquake, Nepal

Journal: Geomorphology

Abstract: Coseismic landslides pose immediate and prolonged hazards to mountainous communities, and provide a rare opportunity to study the effect of large earthquakes on erosion and sediment budgets. By mapping landslides using high-resolution satellite imagery, we find that the 25 April 2015 Mw7.8 Gorkha earthquake and aftershock sequence produced at least 25,000 landslides throughout the steep Himalayan Mountains in central Nepal. Despite early reports claiming lower than expected landslide activity, our results show that the total number, area, and volume of landslides associated with the Gorkha event are consistent with expectations, when compared to prior landslide-triggering earthquakes around the world. The extent of landsliding mimics the extent of fault rupture along the east-west trace of the Main Himalayan Thrust and increases eastward following the progression of rupture. In this event, maximum modeled Peak Ground Acceleration (PGA) and the steepest topographic slopes of the High Himalaya are not spatially coincident, so it is not surprising that landslide density correlates neither with PGA nor steepest slopes on their own. Instead, we find that the highest landslide density is located at the confluence of steep slopes, high mean annual precipitation, and proximity to the deepest part of the fault rupture from which 0.5–2 Hz seismic energy originated. We suggest that landslide density was determined by a combination of earthquake source characteristics, slope distributions, and the influence of precipitation on rock strength via weathering and changes in vegetation cover. Determining the relative contribution of each factor will require further modeling and better constrained seismic parameters, both of which are likely to be developed in the coming few years as post-event studies evolve. Landslide mobility, in terms of the ratio of runout distance to fall height, is comparable to small volume landslides in other settings, and landslide volume-runout scaling is consistent with compilations of data on larger slope failures. In general, the size ratios of landslide source area to full landslide area are smaller than global averages, and hillslope length seems to largely control runout distance, which we propose reflects a topographic control on landslide mobility in this setting. We find that landslide size dictates runout distance and that more than half of the landslide debris was deposited in direct connection with stream channels. Connectivity, which is defined as the spatial proximity of landslides to fluvial channels, is greatest for larger landslides in the high-relief part of the High Himalaya. Although these failures are less abundant than those at lower elevations, they may have a disproportionate impact on sediment dynamics and cascading hazards, such as landslide reactivation by monsoon rainfall and landslide dams that lead to outburst floods. The overall high fluvial connectivity of coseismic landsliding in the Gorkha event suggests coupling between the earthquake cycle and sediment/geochemical budgets of fluvial systems in

the Himalaya.

41. The new landslide inventory of Tuscany (Italy) updated with PS-InSAR: geomorphological features and landslide distribution

Journal: Landslides

Abstract: In this paper, the updating of the landslide inventory of Tuscany region is presented. To achieve this goal, satellite SAR data processed with persistent scatter interferometry (PSI) technique have been used. The updating leads to a consistent reduction of unclassified landslides and to an increasing of active landslides. After the updating, we explored the characteristics of the new inventory, analysing landslide distribution and geomorphological features. Several maps have been elaborated, as sliding index or landslide density map; we also propose a density-area map to highlight areas with different landslide densities and sizes. A frequency-area analysis has been performed, highlighting a classical negative power-law distribution. We also explored landslide frequency for lithology, soil use and several morphological attributes (elevation, slope gradient, slope curvature), considering both all landslides and classified landslide types (flows, falls and slides).

42. Uncertainties of prediction accuracy in shallow landslide modeling: Sample size and raster resolution

Journal: Catena

Abstract: Understanding landslide characteristics such as their locations, dimensions, and spatial distribution is of highly importance in landslide modeling and prediction. The main objective of this study was to assess the effect of different sample sizes and raster resolutions in landslide susceptibility modeling and prediction accuracy of shallow landslides. In this regard, the Bijar region of the Kurdistan province (Iran) was selected as a case study. Accordingly, a total of 20 landslide conditioning factors were considered with six different raster resolutions (10 m, 15 m, 20 m, 30 m, 50 m, and 100 m) and four different sample sizes (60/40%, 70/30%, 80/20%, and 90/10%) were investigated. The merit of each conditioning factors was assessed using the Information Gain Ratio (IGR) technique, whereas Alternating decision tree (ADTree), which has been rarely explored for landslide modeling, was used for building models. Performance of the models was assessed using the area under the ROC curve (AUROC), sensitivity, specificity, accuracy, kappa and RMSE criteria. The results show that with increasing the number of training pixels in the modeling process, the accuracy is increased. Findings also indicate that for the sample sizes of 60/40% (AUROC = 0.800) and 70/30% (AUROC = 0.899), the highest prediction accuracy is derived with the raster resolution of 10 m. With the raster resolution of 20 m, the highest prediction accuracy for the sample size of 80/20% (AUROC = 0.871) and 90/10% (AUROC = 0.864). These outcomes provide a guideline for future research enabling researchers to select an optimal data resolution for landslide hazard modeling.

43. Spatial prediction of flood-susceptible areas using frequency ratio and maximum entropy models

Journal: Geocarto International

Abstract: Modelling the flood in watersheds and reducing the damages caused by this natural disaster is one of the primary objectives of watershed management. This study aims to investigate the application of the frequency ratio and maximum entropy models for flood susceptibility mapping in the Madarsoo watershed, Golestan Province, Iran. Based on the maximum entropy and frequency ratio methods as well as analysis of the relationship between the flood events belonging to training group and the factors affecting on the risk of flooding, the weight of classes of each factor was determined in a GIS environment. Finally, prediction map of flooding potential was validated using receiver operating characteristic (ROC) curve method. ROC curve estimated the area under the curve for frequency ratio and the maximum entropy models as 74.3% and 92.6%, respectively, indicating that the maximum entropy model led to better results for evaluating flooding potential in the study area.

44. Multi-hazard assessment modeling via multi-criteria analysis and GIS: a case study

Journal: Environmental Earth Sciences

Abstract: Multi-hazard assessment modeling comprises an essential tool in any plan that aims to mitigate the impact of future natural disasters. For a particular area they can be generated by combining assessment maps for different types of natural hazards. In the present study, the analytical hierarchy process (AHP) supported by a Geographical Information System (GIS) was utilized to initially produce assessment maps on hazards from landslides, floods and earthquakes and subsequently to combine them into a single multi-hazard map. Evaluation of the reliability of the proposed model predictions was performed through uncertainty analysis of the variables that we used for producing the final model. The drainage basin of Peneus (Pinios) River (Western Peloponnesus, Greece), an area that is prone to landslides, floods and seismic events, was selected for the implementation of the aforementioned approach. Our findings revealed that the high hazard zones are mainly distributed in the western and north-eastern part of the region under investigation. The calculated multi-hazard map, which corresponds to the potential urban development suitability map of the study area, was classified into five classes, namely of very low, low, moderate, high and very high suitability. The most suitable areas for urban development are distributed mostly in the eastern part, in agreement with the low and very low hazard level for the three considered natural hazards. In addition, by performing uncertainty analysis we showed that the spatial distribution of the suitability zones does not change significantly. Ultimately, the final map was verified using the actual inventory of landslides and floods that affected the study area. In this context, we showed that 80% of the landslide occurrences and all the recorded flood events fall within the boundaries of the moderate, low and very low suitability zones. Consequently, the predictive capacity of the applied method is quite good. Finally, the

spatial distribution of the urban areas and the road network were compared with the derived suitability map and the results revealed that approximately 50% of both of them are located within areas susceptible to natural hazards. The proposed approach can be useful for engineers, planners and local authorities in spatial planning and natural hazard management.

45. Flood susceptibility mapping using novel ensembles of adaptive neuro fuzzy inference system and metaheuristic algorithms

Journal: Science of the Total Environment

Abstract: Flood is one of the most destructive natural disasters which cause great financial and life losses per year. Therefore, producing susceptibility maps for flood management are necessary in order to reduce its harmful effects. The aim of the present study is to map flood hazard over the Jahrom Township in Fars Province using a combination of adaptive neuro-fuzzy inference systems (ANFIS) with different metaheuristics algorithms such as ant colony optimization (ACO), genetic algorithm (GA), and particle swarm optimization (PSO) and comparing their accuracy. A total number of 53 flood locations areas were identified, 35 locations of which were randomly selected in order to model flood susceptibility and the remaining 16 locations were used to validate the models. Learning vector quantization (LVQ), as one of the supervised neural network methods, was employed in order to estimate factors' importance. Nine flood conditioning factors namely: slope degree, plan curvature, altitude, topographic wetness index (TWI), stream power index (SPI), distance from river, land use/land cover, rainfall, and lithology were selected and the corresponding maps were prepared in ArcGIS. The frequency ratio (FR) model was used to assign weights to each class within particular controlling factor, then the weights was transferred into MATLAB software for further analyses and to combine with metaheuristic models. The ANFIS-PSO was found to be the most practical model in term of producing the highly focused flood susceptibility map with lesser spatial distribution related to highly susceptible classes. The chi-square result attests the same, where the ANFIS-PSO had the highest spatial differentiation within flood susceptibility classes over the study area. The area under the curve (AUC) obtained from ROC curve indicated the accuracy of 91.4%, 91.8%, 92.6% and 94.5% for the respective models of FR, ANFIS-ACO, ANFIS-GA, and ANFIS-PSO ensembles. So, the ensemble of ANFIS-PSO was introduced as the premier model in the study area. Furthermore, LVQ results revealed that slope degree, rainfall, and altitude were the most effective factors. As regards the premier model, a total area of 44.74% was recognized as highly susceptible to flooding. The results of this study can be used as a platform for better land use planning in order to manage the highly susceptible zones to flooding and reduce the anticipated losses.

46. Disaster damage detection through synergistic use of deep learning and 3D point cloud features derived from very high resolution oblique aerial images, and

multiple-kernel-learning

Journal: Isprs Journal of Photogrammetry and Remote Sensing

Abstract: Oblique aerial images offer views of both building roofs and facades, and thus have been recognized as a potential source to detect severe building damages caused by destructive disaster events such as earthquakes. Therefore, they represent an important source of information for first responders or other stakeholders involved in the post-disaster response process. Several automated methods based on supervised learning have already been demonstrated for damage detection using oblique airborne images. However, they often do not generalize well when data from new unseen sites need to be processed, hampering their practical use. Reasons for this limitation include image and scene characteristics, though the most prominent one relates to the image features being used for training the classifier. Recently features based on deep learning approaches, such as convolutional neural networks (CNNs), have been shown to be more effective than conventional hand-crafted features, and have become the state-of-the-art in many domains, including remote sensing. Moreover, often oblique images are captured with high block overlap, facilitating the generation of dense 3D point clouds - an ideal source to derive geometric characteristics. We hypothesized that the use of CNN features, either independently or in combination with 3D point cloud features, would yield improved performance in damage detection. To this end we used CNN and 3D features, both independently and in combination, using images from manned and unmanned aerial platforms over several geographic locations that vary significantly in terms of image and scene characteristics. A multiple-kernel-learning framework, an effective way for integrating features from different modalities, was used for combining the two sets of features for classification. The results are encouraging: while CNN features produced an average classification accuracy of about 91%, the integration of 3D point cloud features led to an additional improvement of about 3% (i.e. an average classification accuracy of 94%). The significance of 3D point cloud features becomes more evident in the model transferability scenario (i.e., training and testing samples from different sites that vary slightly in the aforementioned characteristics), where the integration of CNN and 3D point cloud features significantly improved the model transferability accuracy up to a maximum of 7% compared with the accuracy achieved by CNN features alone. Overall, an average accuracy of 85% was achieved for the model transferability scenario across all experiments. Our main conclusion is that such an approach qualifies for practical use.

47. Drought monitoring utility of satellite-based precipitation products across mainland China

Journal: Journal of Hydrology

This study mainly evaluated and compared satellite-based quantitative precipitation estimate products (QPEs) for the drought monitoring of mainland China. Two long-term (more than 30 a) satellite-based QPEs, i.e. the Precipitation Estimation from Remotely Sensed Information using Artificial Neural Networks-Climate Data

Record (PERSIANN-CDR) and the Climate Hazards Group InfraRed Precipitation with Station (CHIRPS), and a short-term (18a)QPE, i.e. the Tropical Rainfall Measuring Mission(TRMM) Multi-Satellite Precipitation Analysis (TMPA) 3B42V7 are considered. Two widely used drought indices, the Standardized Precipitation Index (SPI) and the Palmer Drought Severity Index (PDSI), are chosen to evaluate the drought monitoring utility. The 3B42V7 was only evaluated with PDSI due to the short data records. The results show that all the three QPEs perform satisfactorily in the eastern part of China when using both SPI and PDSI. However, their performances for west China could not be clearly determined due to the sparse gauge networks. 3B42V7 features best performance among the three QPEs in the evaluation using PDSI. To further spatiotemporally evaluate the drought utility of the QPEs, four typical drought-affected regions, i.e. northeast China (NEC), Huang-Huai-Hai plain (3HP), southwest China (SWC), and Loess plateau (LP) were extracted from mainland China for specific case studies. Temporally, all three QPEs are able to detect the typical drought of the four regions with both SPI and PDSI, and 3B42V7 presents the least deviation in PDSI estimate. Spatially, both CHIRPS and 3B42V7 accurately catch the spatial centers and extent of the typical drought events, while PERSIANN-CDR could not match the spatial patterns of drought events well. Generally, the long-term PERSIANN-CDR and CHIRPS perform satisfactorily in drought detection and are suitable for drought utility; however, caution should be applied when studying the spatial variation of drought using PERSIANN-CDR. CHIRPS could also be suitable for near-real-time drought monitoring for its shorter time latency of data release. The short-term 3B42V7 also performs well in many cases, and has thus considerable potential for drought monitoring.

48. Landslide susceptibility modeling applying machine learning methods: A case study from Longju in the Three Gorges Reservoir area, China

Journal: Computers & Geosciences

Landslide is a common natural hazard and responsible for extensive damage and losses in mountainous areas. In this study, Longju in the Three Gorges Reservoir area in China wastaken as a case study for landslide susceptibility assessment in order to develop effective risk prevention and mitigation strategies. To begin, 202 landslides were identified, including 95 colluvial landslides and 107 rockfalls. Twelve landslide causal factor maps were prepared initially, and the relationship between these factors and each landslide type was analyzed using the information value model. Later, the unimportant factors were selected and eliminated using the information gain ratio technique.Thelandslidelocationswererandomlydividedintotwogroups:70%fortraininga nd30%forverifying.Two machine learning models: the support vector machine (SVM) and artificial neural network (ANN), and a multivariate statistical model: the logistic regression (LR), were applied for landslide susceptibility modeling (LSM) for each type. The LSM index maps, obtained from combining the assessment results of the two landslide types, were classified into five levels. The performance of the LSMs was evaluated using the receiver operating characteristics curve and Friedman test.

Results show that the elimination of noise-generating factors and the separated modeling of each landslide type have significantly increased the prediction accuracy. The machine learning models outperformed the multivariate statistical model and SVM model was found ideal for the case study area.